VOL. 13, NO. 15, AUGUST 2018 ISSN 1819-6608
ARPN Journal of Engineering and Applied Sciences

www.arpnjournals.com

THE OPTIMIZATION OF POWER GENERATION IN LOW-COST MASS-PRODUCED WHEELED WIND TURBINES

Luca Piancastelli[1], Alberto Pirazzini[1], Marco Cremonini[2], Stefano Cassani[3], Federico Calzini[3] and Eugenio Pezzuti[4]
[1]Department of Industrial Engineering, Alma Mater Studiorum University of Bologna, Viale Risorgimento, Bologna, Italy
[2]Nuovamacut Automazione SpA, Team System, Via E. Majorana, Reggio Emilia, Italy
[3]MultiProjecta, Via Casola Canina, Imola, Italy
[4]Università di Roma "Tor Vergata", Dip. di Ingegneria dell'Impresa "Mario Lucertini", Via del Politecnico, Roma, Italy
E-Mail: luca.piancastelli@unibo.it

ABSTRACT

In fixed wind turbine installations, the optimal wind location is difficult to individuate, permissions are difficult to obtain and the production site is distant from the costumers. The large production scale of small wheeled wind turbines keep the cost at minimum and give the possibility to install the windmill close to the final costumers. CFD simulation makes it possible to optimize the matching of a small mobile wind turbine with an automotive commercial alternator. This paper proposes an innovative device to furl the wind turbine around the pole axis in such a way to optimize energy production and avoid over-speed. For this purpose a commercial shock-absorber and a cam mechanism are used. The CFD simulation, in this case with Flow Simulation of Solid Works, makes it possible to design the turbine, the tail vane and the mechanism to maximize energy production. The device includes a shock absorber and a cam mechanism. The system provides optimum matching of the turbine torque output to the generator shaft. The same mechanism also determines the cut-out speed. The automotive generator includes a system to charge a 24V standard battery. Then, a power inverter outputs the electric energy to the grid. The 4m-diameter three-blades-rotor is connected to the 3.6kW automotive alternator through a commercial 2.5:1 speed multiplier.

Keywords: wind turbine, energy production, low cost, generator matching, cam furling mechanism.

INTRODUCTION

The Betz formula for power P_{max} in the wind is (1) [0].

$$P_{Betz} = \frac{16}{27} P_{wind} = \frac{2}{27} \pi \rho D^2 v^3 \quad (1)$$

In our case the nominal wind speed v is 10 m/s and air density ρ=1.225 and P_{Betz}=4.5 kW. However, the cut-out velocity is 100 km/h and the Betz's power is approximately P_{max}≈100 kW. The variation between the power at the nominal speed and the maximum one is then (1):

$$\Delta P = \frac{P_{\max} - P_n}{P_n} 100 \approx 2000[\%] \quad (2)$$

In fact, because of this cubic relationship with v, the power availability is extremely sensitive to wind speed.

The true variation is even larger, in our case the cut-in speed is the highest velocity of "light air" in the Beaufort scale that corresponds to 2.5 m /s. The Betz's ΔP is then about 2200%.

This extreme variability influences all aspects of system design. It makes it difficult to consider trying to use winds of less than 2.5m/s since the power available is too small, while it becomes essential to shed power of the windmill down if the wind speed exceeds about 12m/s as excessive power then becomes available which would overstress the windmill structure and exceed the electrical generator capability. This is true at sea level ISA+0 (15 °C). The power in the wind is a function of the air-density, so it declines increasing altitude and temperature. An approximate model of the ISA (International Standard Atmosphere) can be obtained by equations (3) (4) and (5) [1].

$$T = T_0 - 6.5 \frac{h}{1000} \quad (3)$$

$$p = p_0 - \left(1 - 0.0065 \frac{h}{T_0}\right)^{5.2561} \quad (4)$$

$$\rho = \frac{p}{RT} \quad (5)$$

Figure-1 shows the variation of density with altitude (m) and temperature (DEG Celsius).

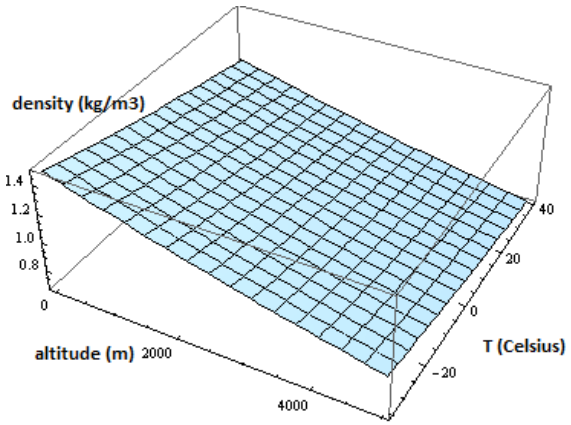

Figure-1. Density vs. T and altitude.

The effect of altitude and temperature is relatively small, when compared with wind velocity. For example, the relative variation of power in the wind from -35C/a.s.l. to 40C/5000m is (6):

$$\Delta\rho = \frac{\rho_{-35,0} - \rho_{40}}{\rho_{40}} \approx 25\% \quad (6)$$

The effect of altitude (Figure-2) is more important than temperature (Figure-3). The total combined of environmental data (altitude and temperature) and velocity varies the power in the wind up to "only" 20 times.

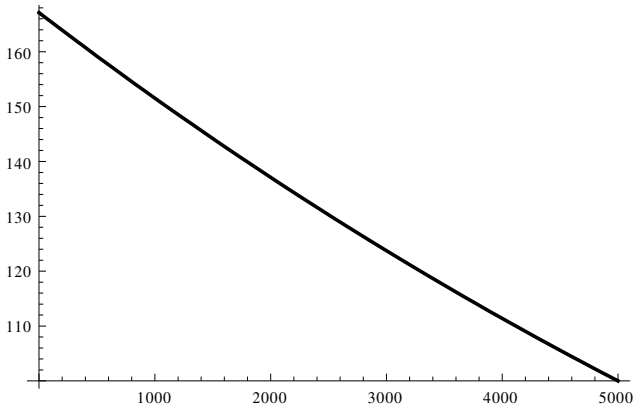

Figure-2. Density (%) vs. altitude (m).

However, due to the cube law, the power in the wind is much more sensitive to velocity rather than to air density. For example, a wind speed of 5.64m/s at 3,000m equals the power density of a 5m/s wind at sea level. Therefore, quite a marginal increase in wind velocity compensates the density drop of high altitudes. Typically, due to the cubic law, the fluctuations in the wind speed result in the average power-in-the-wind being from1.5 up to 3 times the one that occurs at the mean wind speed.

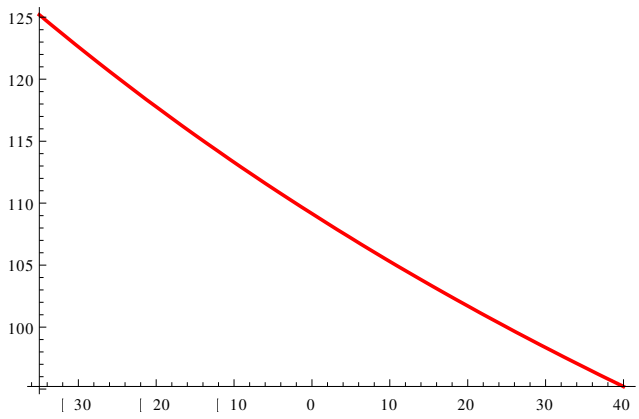

Figure-3. Density (%) with OAT (outside air temperature) (Celsius).

However, for practical calculations, the energy available is the mean wind speed cubed. There mechanism for converting the kinetic energy of the wind into mechanical work is to slow the wind by producing lift, thereby extracting kinetic energy. In most windmills, an airfoil or a flat surface forms a small angle to the wind to produce lift. This deflects the velocity vector and produces a force perpendicular and a drag force parallel to the vector. Blade optimization consists in producing little turbulence to increase efficiency. The Betz's law of expression (1) limits the power extraction to about 60%. This is because the windmill cannot stop the wind. The turbo-lag of the wind turbine with wind fluctuations may be evaluated by a sheer energy balance. Expressions (7) (8) (9) and (10) can be used for an initial evaluation of rotor diameter D, wind velocity v and polar inertia moment of rotor J for a horizontal axis windmill of power P.

$$P = 310D^{2.1} \quad (7)$$

$$P = \eta_T P_{Betz} \cong \eta_T \frac{2}{27}\pi\rho D^2 v^3 \quad (8)$$

$$J = 0.0374D^{4.13} \quad (9)$$

For a power of 3 kW, a rotor can have λ=6 and η_T=0.7. In this case, it will require a wind velocity v=11.6 m/s, D≈3 m, J=4 kg*m^2. In this case the energy contents of the wind and the rotor can be calculated with equations (10) and (11).

$$E_{wind} = \frac{\rho\pi D^2 v^3}{8} \approx 8000 \quad (10)$$

$$E_{rotor} = \frac{J\omega^2}{2} = \frac{J\lambda^2 v^2}{8D^2} \approx 4000 \quad (11)$$

The turbo-lag is then minimum. This is due to the larger amount of power of the wind when compared with

the inertia of the windmill. The regulation system needed to control the windmill should then be very fast to avoid over speeds. Free windmill regulation systems tends to stay very well inside the safety region cutting the input power well before any risk of damage may arise. However the cut-in velocity is extremely critical, since the still windmill does not generate any energy. For this reason the design of a windmill, even a very large and well controlled one is usually a compromise.

It is possible to plot experimentally derived curves of output power (red, Figure-4) against rotational speed at various wind speeds. Similarly the torque produced by the turbine is shown (black, Figure-4).

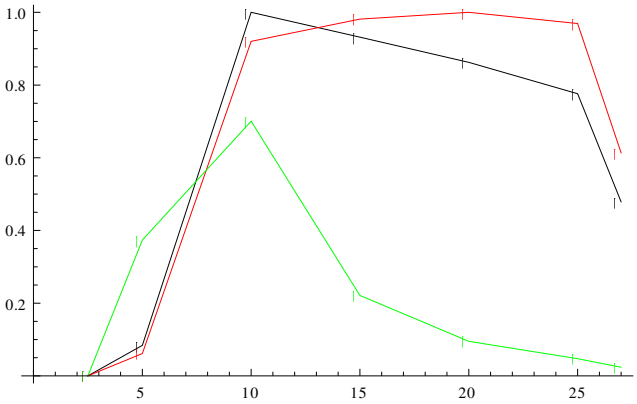

Figure-4. Characteristic curves of a 1.5 MW wind turbine vs. speed (m/s). Red curve is Power/P_n, black curve is Torque/T_{max}. Green curve is efficiency.

Finally, the efficiency is represented (green, Figure-4). The maximum efficiency coincides with the maximum power output in a given wind speed. Conventionally, in windmills efficiency is usually presented as the "Power Coefficient" or Cp. This is a non-dimensional ratio of shaft-power divided by the Betz's maximum power through a shape having the same area as the vertical profile of the windmill rotor. Figure-4 shows a few very interesting design features. This 1.5 MW turbine has the blade controlled in pitch. It is paramount for the design to have a fairly low cut-in speed (2.5 m/s). Then the power curve follows a nearly cubic low up to the nominal design condition (10 m/s, 1.5 MW). After this value the control system has to increase the pitch in order to keep the torque nearly constant up to the cut-out wind feather speed (25 m/s). This turbine has a good peak efficiency η_T of nearly 70%. This value may appear low, but for the propeller-generator assembly is a good value. It is necessary to understand that the design of large propellers in windmill-mode is not easy and faces several constraints. It should work in any weather condition including rain and the long blades have stress and flutter/vibration problems. After the nominal power is reached the power is cut by the control system not to overload the generator and the electric network. Near constant rotational speed is kept from 10 m/s to 25 m/s, to avoid overstressing of the rotor. In this very large machine the control system is a fundamental and expensive part of the wind power unit. The nominal rotational design speed is also conventionally expressed non-dimensionally as the "tip-speed ratio". This coefficient λ is the ratio of the speed of the windmill rotor tip, at radius R when rotating at ω rad/s, to the speed of the wind*v*.

When the turbine is stationery, λ is zero, and the blades are stalled. This occurs when the torque produced by the wind on the turbine shaft is below the level needed to overcome the resistance of the starting load.

In rotors, the windmill mode starts at lower wind velocity for straight bladed rotors with many blades. This is the case of traditional Bevil's windmills (US 226,265 patent, 1880), where high torques are required at low wind speeds with nearly constant torque required by the pump. In this windmill many very simple flat blades are used to achieve this result. This concept is called solidity. In horizontal propeller windmills, "Solidity" is the proportion of a windmill rotor's swept area that is filled with solid blades by looking at the rotor along the rotation axis. It is conventionally defined as the ratio of the sum of the mean-airfoil-chords of all the blades to the circumference of the rotor. This value is conventionally measured at blade tip. Multi-bladed rotors, typical on wind-pumps have high "solidity", because a large proportion of the rotor swept area is "solid" with blades. Wind-pumps run at low speeds and high starting torque. Therefore, the pitch is large. This gives it a tip-speed ratio at its maximum efficiency, of around 1.25, with low maximum coefficient of performance. However, the multi-bladed rotor has a higher torque coefficient at zero tip-speed ratio (0.5 - 0.6) than many of the other types. The high starting torque is higher than the running torque and the slow speed of rotation in a given wind match the reciprocating borehole pump torque curve. In contrast, the two or three-bladed, low-solidity, twisted blades rotors are the most efficient. However, rotor tips travels at six to ten times the speed of the wind to achieve their best efficiency. To do so the pitch is very small, the velocity vector has a large angular deviation and the rotor spins much faster for a given wind-speed than a high solidity rotor. Unfortunately, low solidity rotors have an extremely small starting torque, which means they can only match loads which require a nearly null torque to start them, like certain types of electric generators and centrifugal pumps. To extract the maximum energy from a wind turbine requires a shaft load which causes the operating point to follow close to the locus of maximum power and torque. Theoretically also the maximum efficiency of the generator should be searched for. This is possible in the constant speed generators, like the one of figure 4. However in smaller wind-turbines it is difficult to achieve, since the control system and the mechanism are quite expensive and should be absolutely reliable with the cubic power law of the wind energy. Also the velocity of the controls should be extremely high, since and over speed of 40% more than doubles the stress. In fact, the centrifugal force follows a quadratic law. The "matching efficiency", is actually less serious than it may seem, since the best efficiency is truly needed only at low wind-speeds. When a wind turbine is running fast enough to be badly matched with its load, it means that the wind speed

is high and the bad matching reduces the excess of rotor speed/torque that cannot be transformed in useful energy and it is also of potential damage to the windmill itself.

Theoretically, when generators are used as load, instead of pumps, a much better match can be obtained. There is considerable advantage in improving the overall performance of wind generators by developing methods of improving the rotor-to-generator match over a wider range of wind-speeds. But in the meantime the main problem is to choose the most convenient generator for a given windmill in a given wind regime. The most convenient generators available are the heavy automotive ones for passenger coaches and heavy rig-transporters. These generators include a system to charge the batteries. The mass production in millions of items reduces the costs substantially. Therefore, the system is extremely economical. However, automotive generator output depends on rpm and battery charging voltage. Typical curves for an automotive generator are shown in Figure-5.

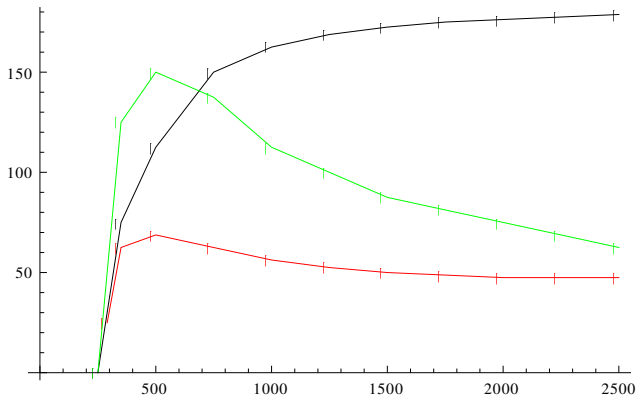

Figure-5. Automotive generator curves vs. rpm. Black is current (A). Red is efficiency. Green is torque (Nm*50).

Therefore, with an automotive generator there is an important trade-off between achieving starting in adequately light winds and achieving a good output.

The operating characteristic of a typical automotive generator (Figure-4) shows that the windmill should reach its best match with the generator close to 750 rpm. This generator-shaft rpm should be obtained at the "Nominal or Design Wind-speed". Then the wind turbine increases its output only slightly up to 2.500 rpm (its cut-out speed). At higher wind-speeds, means must be introduced to prevent it speeding up further, or the over-speed will damage the generator. Therefore it is strictly necessary to make the windmill "feather", "reef", "furl" or "shut- down". Various known methods for cut-out are discussed in the next section.

Methods of storm protection and furling

In fact, because of this cubic relationship with v, windmills must have a means to limit the power they can deliver to avoid overstress and damage.

Ancient windmills use fewer sails in high winds or else the sails are partially rolled around their spars. In metal and composite small windmills (Bevil's patent US 226, 265, 1880), the rotor axis has an offset from the tower centre so that the wind constantly seeks to turn the rotor behind the tower. Under normal conditions the rotor is held normal to the wind by a long tail with a vane on it. This vane is hinged, and held in place by a pre-loaded spring. When the wind pressure on the rotor disk reaches overcomes the pre-tension in the spring, the tail will fold until the wind pushes the rotor parallel to the wind. This furling process increases progressively until the machine is fully furled.

Wind-generators and other wind-turbines with high speed, low-solidity rotors often use a mechanism which changes the blade pitch. The pitch variation may be electric or hydraulic powered and it is controlled by a computer. In a pure mechanical version it has small counter-weights near the rotor hub, which force the blades to feather under the influence of centrifugal force when the rotor reaches its furling speed. The return to the nominal pitch is assured by the force of an elastic system enclosed in the hub. A few turbines deploy air-brake flaps to prevent over-speed.

The market

Siting is most critical to the success of an effective installation. The wind turbine, even when it is a small power, is a complex system, consisting of the windmill, the wind and the local microclimate and the regulatory framework within which it is positioned. The mini and micro machines enlist a potentially huge market. For this reason it is extremely important to contain purchase and maintenance costs through off-the-shelf mass produced components.

Success factors for the future of micro and small wind turbines are essentially attributable to the identification of technological solutions specifically addressed to the segments of the market and the available resource. This concept is also part of the effective machines at sites with low noise to be usable. Reduction of construction costs is obtained by large-scale production and modular design. The wind turbine must have high reliability. The fail safe design ensures safety to persons and the integrity of the goods nearby the installation. Finally, low installation and maintenance costs are required [1-18].

THE NEW CONCEPT: A MOBILE WIND TURBINE

The 4m-diameter three-blades-rotor moves an automotive alternator through a commercial speed multiplier. The alternator charges a battery. A power inverter outputs the electric energy to the grid.

A commercial low-cost wheeled trailer supports the windmill. Even a small car without special driving license can pull the loaded trailer. Therefore, the maximum allowed mass for the windmill and the trailer is less than 750 kg. The maximum dimensions are of 4,000mm in length and 1,400 mm for width.

An electrically actuated hydraulic system deploys the windmill. The vehicle battery can power the process. Foundations and permissions are not necessary. The trailer is equipped with telescopic arms to improve stability.

The serial production concept, the simple structure and the extensive use of commercial components guarantees economy and environmental friendliness.

The automotive generator limits the theoretical maximum power output to4, 000W [18-27].

Necessity and methods for regulating rotational speed

Horizontal wind turbines should operate in a wide range of wind speeds, but are truly efficient when operating in winds near their rated wind speed. At higher and lower velocity the aim is to maximize generator performance that to extract the most of the wind power. A turbine with afixed blade pitch, left unregulated, finds its minimum energy condition. It then rotates at a slower speed under slower wind speeds and rotates much faster at wind speeds larger than the rated wind speed. Both cases prevent direct power output into a power grid because the generator would produce power with a frequency and a voltage that changes with wind speed. This is not acceptable because frequency and voltage are strictly tolerance by the electric power Authority. To rectify this problem there exist several methods for regulating a turbine's output power: yaw control, mechanical and electrical braking, variable speed operation, stall control, and pitch control.

The new regulation system

Increasing the yaw angle between the turbine axis and the incident wind results in a power reduction approximately proportional to the cube of the cosine of the wind. Therefore, an increase of the yaw angle at wind speeds higher than the nominal one reduces the turbine output power. However, it results in unequal forces and wind velocities acting on the rotor and on the blades throughout its rotation. This causes the rotor to wobble due to aerodynamic loads and subjects it to greater fatigue stress. This problem is important in large turbine were the blades are several meters long. In mini and micro turbines are far stiffer in bending. In fact the blades behave like a cantilever beam whose stiffness is inversely proportional to the cube of the length. For the 4 kW wind turbine of this work the yaw regulation is then possible. The main issue is the matching between the automotive generator of (Figure-5) and the windmill. The matching should be economical, reliable, fail safe and efficient. The nominal speed of the generator can be very low. In fact, the generators output 150A (3.6 kW) at 750 rpm. It is then possible to have an over speed of the alternator of 233% (12). Since wind torque and windmill rpm follow a quadratic law, the allowed over speed before the generator reaches its maximum (2500 rpm) will be of about 50%. This choice allows a safety margin, since turbine efficiency fades with speed.

$$overspeed = \frac{v_{max} - v_n}{v_n} \approx 233\% \quad (12)$$

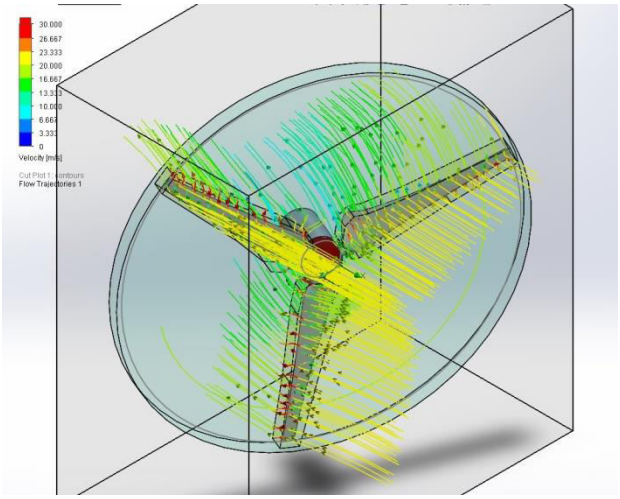

Figure-6. Flow simulation of the turbine.

From equation (7) it is possible to calculate an approximate diameter of the wind turbine. However, the automotive alternator has a low efficiency η_G=0.50, while windmill alternators reach easily η_G=0.8. Therefore, the evaluation of equation (7) should be done with P_n=5.1kW instead of P_n=3.2kW. A possible diameter is then D=4m. A nominal wind v=11 m/s velocity comes from the turbine efficiency (overall with the speed multiplier without the generator) η_{TM}=0.7. It is then possible the design of the blades and to optimize them with Solid Works Flow Simulation. The pressure pattern on the blades is a good parameter for this optimization. After the optimization the nominal wing speeds is about v_n=11.5m/s at 300rpm (turbine shaft). The transmission ratio is then 750/300=2.5 and the cut-out velocity is 1.5 times v_n (17m/s).

The software accuracy is pretty good. However, the final evaluation requires experimental tests. The worst condition for the furling system is with the maximum air density (ISA -50@s.l.). It is then possible to evaluate the turbine speed and force on disk for each yaw angle (Table-1).

Table-1. Force normal to rotor disk (N).

	Yaw angle DEG	**0**	**22.5**	**4.5**	**67.5**	**90**
v (m/s)						
10		686	403	185	24	≈0
13		1160	682	310	42	≈0
16		1760	1034	470	67	≈0
19		2483	1459	658	95	≈0
22		3334	1944	877	138	≈0

If the turbine offset from the pole axis is 100m, it is possible to evaluate the bending moment and to evaluate the minimum size for the tail vane. It is then possible to simulate the assembly to find the stable configuration for each wind velocity (Figure-8).

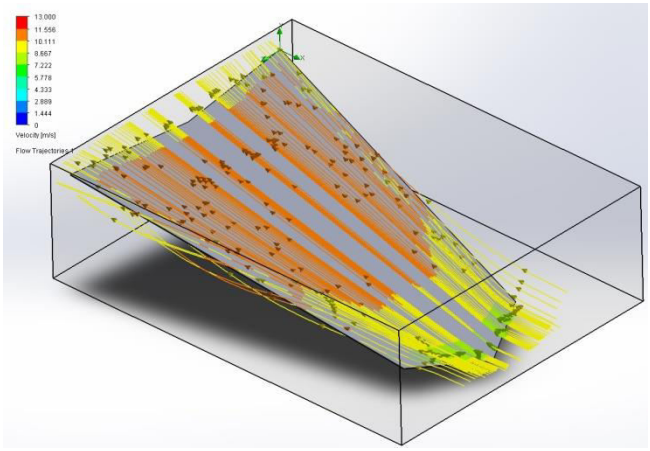

Figure-7. Flow simulation of the tail vane.

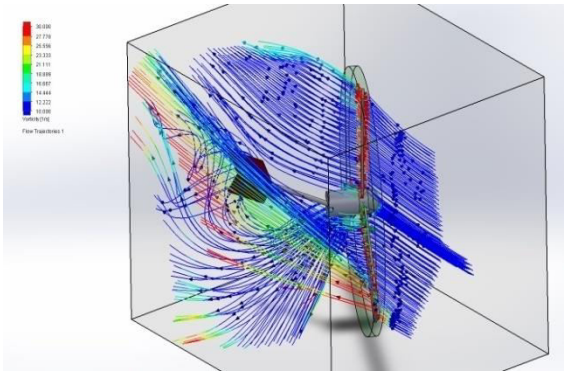

Figure-8. Stable aerodynamic configuration.

In order to obtain the desired configuration for each wind velocity a mechanical device was designed. This device is composed by a commercial shock absorber and a cam mechanism. The optimum position for the shock absorber and the preload and stiffness curve of the spring are calculated as a first step. This device is shown in figure 9. The shock absorber has a stroke of 75mm and an eye-to-eye length of 240mm.

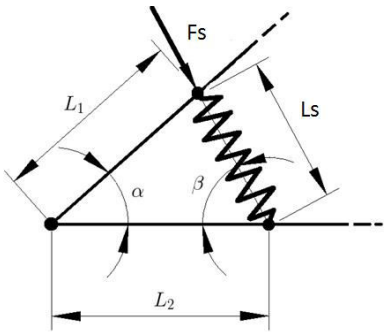

Figure-9. Spring mechanism for yaw control.

L_1=234mm, L_2=50mm, k=N/mm and L_0=295 can be calculated from Equations (13) (14) and (15).

$$Ls = \sqrt{(L_2 - L_1 \cos\alpha)^2 + (L_1 \sin\alpha)^2} \quad (13)$$

$$Fs = k(Ls - Ls_0) \quad (14)$$

$$\beta' = ArcTan\left(\frac{L_1 \sin\alpha}{L_2 - L_1 \cos\alpha}\right) \quad (15)$$

The moment on the turbine is then (16):

$$M = L_1 F_s \sin(\pi - \alpha - \beta) = L_1 k(Ls - Ls_0)\sin(\pi - \alpha - \beta) \quad (16)$$

The curve obtained (Figure-10) in this way is not the one necessary to match the automotive generator of Figure-5.

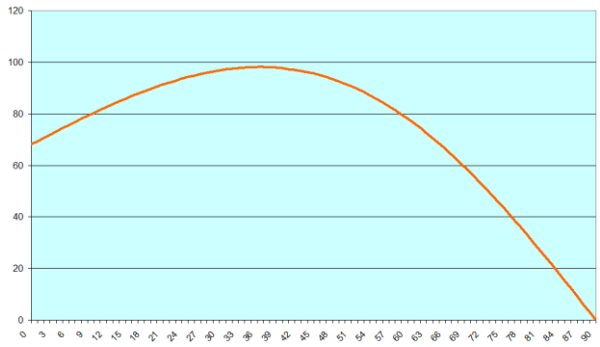

Figure-10. Moment (Nm) vs. α (DEG) for the mechanisms of Figure-9.

A cam mechanism should then be added (Figure 11).

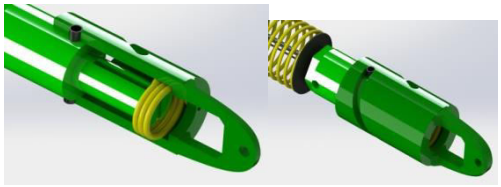

Figure-11. Cam mechanism.

A torsion spring forces the shock absorber head at a defined length through a cam mechanism that is based on the rotation of the piston rod. Figure-12 shows the assembled yaw control mechanism.

CONCLUSIONS

CFD simulation makes it possible to optimize the matching of a small mobile wind turbine with an automotive commercial alternator. This paper proposes an innovative device to furl the wind turbine around the pole axis in such a way to optimize energy production and avoid over-speed. For this purpose a commercial shock-absorber and a cam mechanism were used. The CFD simulation, in this case with Flow Simulation of Solid Works, makes it possible to design the turbine, the tail vane and the mechanism to maximize energy production. The automotive generator includes a system to charge a 24V standard battery. Then, a power inverter outputs the electric energy to the grid. The 4m-diameter three-blades-

rotor is connected to the 3.6kW automotive alternator through a commercial 2.5:1 speed multiplier. A commercial low-cost wheeled trailer supports the windmill. Even a small car without special driving license can pull the loaded trailer. Therefore, the maximum allowed mass for the windmill and the trailer is less than 750 kg. The maximum dimensions are of 4,000mm in length and 1,400 mm for width.

An electrically actuated hydraulic system deploys the windmill. The vehicle battery can power the process. Foundations and permissions are not necessary. The trailer is equipped with telescopic arms to improve stability. Sitting is then optimized by moving the windmill.

Figure-12. Wind turbine assembly.

REFERENCES

[1] L. Piancastelli, L. Frizziero, S. Marcoppido, E. Pezzuti. 2012. Methodology to evaluate aircraft piston engine durability. edizioni ETS. International Journal of Heat & Technology. ISSN 0392-8764, 30(1): 89-92, Bologna.

[2] L. Piancastelli, L. Frizziero, G. Donnici. 2015. The Meredith ramjet: An efficient way to recover the heat wasted in piston engine cooling. Asian Research Publishing Network (ARPN). Journal of Engineering and Applied Sciences. ISSN 1819-6608, 10(12): 5327-5333, EBSCO Publishing, 10 Estes Street, P.O. Box 682, Ipswich, MA 01938, USA.

[3] L. Piancastelli, A. Gatti, L. Frizziero, L. Ragazzi, M. Cremonini. 2015. CFD analysis of the Zimmerman's V173 stol aircraft. Asian Research Publishing Network (ARPN). Journal of Engineering and Applied Sciences. ISSN 1819-6608, 10(18): 8063-8070, EBSCO Publishing, 10 Estes Street, P.O. Box 682, Ipswich, MA 01938, USA.

[4] L. Piancastelli, L. Frizziero. 2014. Turbocharging and turbocompounding optimization in automotive racing. Asian Research Publishing Network (ARPN). Journal of Engineering and Applied Sciences. ISSN 1819-6608, 9(11): 2192-2199, EBSCO Publishing, 10 Estes Street, P.O. Box 682, Ipswich, MA 01938, USA

[5] L. Piancastelli, L. Frizziero, G. Donnici. 2014. The common-rail fuel injection technique in turbocharged di-diesel-engines for aircraft applications. Asian Research Publishing Network (ARPN). Journal of Engineering and Applied Sciences. ISSN 1819-6608, 9(12): 2493-2499, EBSCO Publishing, 10 Estes Street, P.O. Box 682, Ipswich, MA 01938, USA

[6] L. Piancastelli, L. Frizziero, G. Donnici. 2015. Turbomatching of small aircraft diesel common rail engines derived from the automotive field. Asian Research Publishing Network (ARPN). Journal of Engineering and Applied Sciences. ISSN 1819-6608, 10(1): 172-178, EBSCO Publishing, 10 Estes Street, P.O. Box 682, Ipswich, MA 01938, USA

[7] L. Piancastelli, L. Frizziero. 2015. Supercharging systems in small aircraft diesel common rail engines derived from the automotive field. Asian Research Publishing Network (ARPN). Journal of Engineering and Applied Sciences. ISSN 1819-6608, 10(1): 20-26, EBSCO Publishing, 10 Estes Street, P.O. Box 682, Ipswich, MA 01938, USA

[8] P.P.Valentini, E. Pezzuti E. Computer-aided tolerance allocation of compliant ortho-planar spring mechanism. Int. Jou. of computer applications in technology, 53: 369-374, ISSN: 0952-8091, doi: 10.1504/IJCAT.2016.076801

[9] E. Pezzuti, PP. Valentini PP. Accuracy in fingertip tracking using Leap Motion Controller for interactive virtual applications. Int. Jour. On interactive design and manufacturing, pp. 1-10, ISSN: 1955-2513, doi: 10.1007/s12008-016-0339-y.

[10] E.Pezzuti E, PP. Valentini P. Design and interactive simulation of cross-axis compliant pivot using dynamic spline. Int. Jour. On interactive design and manufacturing, 7: 261-269, ISSN: 1955-2513, doi: 10.1007/s12008-012-0180-x

[11] L. Piancastelli, S. Cassani. 2017. Maximum peak pressure evaluation of an automotive common rail

diesel piston engine head. Asian Research Publishing Network (ARPN). Journal of Engineering and Applied Sciences. ISSN 1819-6608, 12(1): 212-218, EBSCO Publishing, 10 Estes Street, P.O. Box 682, Ipswich, MA 01938, USA.

[12] S. Cassani. 2017. Airplane design: the superiority of fsw aluminum-alloy pure monocoque over cfrp "black" constructions. Asian Research Publishing Network (ARPN). Journal of Engineering and Applied Sciences. ISSN 1819-6608, 12(2): 377-361, EBSCO Publishing, 10 Estes Street, P.O. Box 682, Ipswich, MA 01938, USA.

[13] L. Piancastelli, S. Cassani. 2017. Power speed reduction units for general aviation part 2: general design, optimum bearing selection for propeller driven aircrafts with piston engines. Asian Research Publishing Network (ARPN). Journal of Engineering and Applied Sciences. ISSN 1819-6608, 12(2): 544-550, EBSCO Publishing, 10 Estes Street, P.O. Box 682, Ipswich, MA 01938, USA.

[14] L. Piancastelli, S. Cassani. 2017. Power Speed Reduction Units For General Aviation Part 5: Housing/Casing Optimized Design For Propeller-Driven Aircrafts And Helicopters. Asian Research Publishing Network (ARPN). Journal of Engineering and Applied Sciences. ISSN 1819-6608, 12(2): 602-608, EBSCO Publishing, 10 Estes Street, P.O. Box 682, Ipswich, MA 01938, USA.

[15] L. Piancastelli, S. Cassani. 2017. Power speed reduction units for general aviation part 3: simplified gear design piston-powered, propeller-driven general aviation aircrafts. Asian Research Publishing Network (ARPN). Journal of Engineering and Applied Sciences. ISSN 1819-6608, 12(3): 870-874, EBSCO Publishing, 10 Estes Street, P.O. Box 682, Ipswich, MA 01938, USA.

[16] L. Piancastelli, S. Cassani. 2017. Power speed reduction units for general aviation part 4: simplified gear design for piston-powered, propeller-driven heavy duty aircrafts and helicopters. Journal of Engineering and Applied Sciences. ISSN 1819-6608, 12(5): 1533-1539, EBSCO Publishing, 10 Estes Street, P.O. Box 682, Ipswich, MA 01938, USA.

[17] L. Piancastelli, S. Migliano, S. Cassani. 2017. An Extremely Compact, High Torque Continuously Variable Power Transmission for large hybrid terrain vehicles. Journal of Engineering and Applied Sciences. ISSN 1819-6608, 12(6): 1796-1800, EBSCO Publishing, 10 Estes Street, P.O. Box 682, Ipswich, MA 01938, USA.

[18] L. Piancastelli, S. Cassani. 2017. Mapping Optimization For Partial Loads Of Common Rail Diesel Piston Engines. Journal of Engineering and Applied Sciences. ISSN 1819-6608, 12(7): 2223-2229, EBSCO Publishing, 10 Estes Street, P.O. Box 682, Ipswich, MA 01938, USA.

[19] L. Piancastelli, S. Cassani. 2017. High altitude operations with piston engines power plant design optimization part v: nozzle design and ramjet general considerations. Journal of Engineering and Applied Sciences. ISSN 1819-6608, 12(7): 2242-2247, EBSCO Publishing, 10 Estes Street, P.O. Box 682, Ipswich, MA 01938, USA.

[20] L. Piancastelli, R. V. Clarke, S. Cassani. 2017. Diffuser augmented run the river and tidal picohydropower generation system. Journal of Engineering and Applied Sciences. ISSN 1819-6608, 12(8): 2678-2688, EBSCO Publishing, 10 Estes Street, P.O. Box 682, Ipswich, MA 01938, USA.

[21] L. Piancastelli, M. Gardella, S. Cassani. 2017. Cooling system optimization for light diesel helicopters. Journal of Engineering and Applied Sciences. ISSN 1819-6608, 12(9): 2803-2808, EBSCO Publishing, 10 Estes Street, P.O. Box 682, Ipswich, MA 01938, USA.

[22] L. Piancastelli, S. Cassani. 2017. Study and optimization of a contra-rotating propeller hub for convertiplanes. Part 1: vto and hovering. Journal of Engineering and Applied Sciences. ISSN 1819-6608, 12(11): 3451-3457, EBSCO Publishing, 10 Estes Street, P.O. Box 682, Ipswich, MA 01938, USA.

[23] L. Piancastelli, S. Cassani. 2017. On the conversion of automotive engines for general aviation. Journal of Engineering and Applied Sciences. ISSN 1819-6608, 12(13): 4196-4203, EBSCO Publishing, 10 Estes Street, P.O. Box 682, Ipswich, MA 01938, USA.

[24] L. Piancastelli, S. Cassani. 2017. Convertiplane cruise performance with contra-rotating propeller. Journal of Engineering and Applied Sciences. ISSN 1819-6608, 12(19): 5554-5559, EBSCO Publishing, 10 Estes Street, P.O. Box 682, Ipswich, MA 01938, USA.

[25] L. Piancastelli, S. Cassani. 2017. Tribological problem solving in medium heavy duty marine diesel

engine part 1: journal bearings. Journal of Engineering and Applied Sciences. ISSN 1819-6608, 12(22): 6533-6541, EBSCO Publishing, 10 Estes Street, P.O. Box 682, Ipswich, MA 01938, USA.

[26] A. Ceruti, T. Bombardi, T., L. Piancastelli. 2016. Visual Flight Rules Pilots Into Instrumental Meteorological Conditions: a Proposal for a Mobile Application to Increase In-flight Survivability. International Review of Aerospace Engineering (IREASE). 9(5).

[27] L. Piancastelli, A. Burnelli A., S. Cassani. 2017. Validation of a simplified method for the evaluation of pressure and temperature on a RR Merlin XX head, International Journal of Heat and Technology, Vol. 35, No. 1, pp. 549558. DOI: 10.18280/ijht.350311.

Symbol	Description	Unit
P_{Betz}	Betz's Power (1)	W
P_{wind}	Wind Power	W
ρ	Air density	kg/m^3
D	Turbine diameter	m
v	Wind speed	m/s
P_{max}	Max Betz's power	W
P_n	Nominal Betz's power	W
T	ISA Temperature	K
T_0	Ref. Air Temperature	K
p	ISA Pressure	Pa
P_0	Ref pressure	Pa
h	Altitude	m
η_T	Turbine efficiency	-
J	Turbine polar inertia moment	kg*m2
λ	Velocity ratio	-
v_{max}	Max allowed v	m/s
v_n	Nominal v	m/s
L_i	See Figure 9	m
L_0	Spring free length	m
Fs	Spring Force	N
k	Spring stiffness	N/mm